Astron. Astrophys. 237, 61–72 (1990)

ASTRONOMY AND ASTROPHYSICS

Red giants in open clusters

III. Binarity and stellar evolution in five intermediate-age clusters: NGC 2360, 2423, 5822, 6811 and IC 4756*

J.-C. Mermilliod[1] **and M. Mayor**[2]

[1] Institut d'Astronomie de l'Université de Lausanne, CH-1290 Chavannes-des-Bois, Switzerland
[2] Observatoire de Genève, CH-1290 Sauverny, Switzerland

Received February 5, accepted March 28, 1990

Abstract. Coravel radial velocities of 93 red giants in five open clusters older than the Hyades (NGC 2360, 2423, 5822, 6811 and IC 4756) are analyzed for membership and binary detection. Seventeen binaries have been discovered among the 71 members, resulting in a binary percentage of 27%. One new orbit has been determined in IC 4756, with a long period (2000 days) and a very small eccentricity ($e=0.04$).

The cluster ages are around 2.2 10^9 yr ($9.3<\log t<9.4$), and the masses at the end of the main sequence are between 1.8 and 1.9 $M_\odot$. The colour-magnitude diagrams of the red giants, displaying clumps and not long giant branches, imply that the stars do not evolve through helium flash. Therefore the limiting initial stellar mass for helium ignition in non-degenerate cores must be smaller than the standard value of 2.2 $M_\odot$. The isochrone fitted in the diagram of NGC 2360 shows that the evolutionary models with core overshooting reproduce the observations better than the standard models (without overshooting) do, and that the structure of the red giant track can be described observationally. This also confirms the general morphology already found in the five Hyades-generation clusters and supports the previous detection of a concentration of stars about 0.2 to 0.4 mag below the clump.

Key words: open clusters – red giants – spectroscopic binaries – stellar evolution

1. Introduction

This is the third paper in the series devoted to the study of red giants in open clusters which started with the study of five Hyades-generation open clusters (Mermilliod and Mayor, 1989, Paper I) and the publication of the orbits of ten spectroscopic binaries (Mermilliod et al., 1989, Paper II). We make use of Coravel radial-velocity observations to eliminate the non-member stars and detect binaries and new data in the Geneva photometric system to study the distribution of the red giants in the colour-magnitude diagrams of intermediate-age clusters. By observing stars in clusters of the Hyades generation and older, hence covering the right age range, we hope to define the limiting mass below which stars develop a degenerate helium core and evolve through helium flash. At this limit a profound change occurs in the morphology of the giant branch (Barbaro and Pigatto, 1984). Overshooting is believed to bring this limiting mass below 2.2 $M_\odot$ because it produces an increase of the size of the convective core. In Paper I (Mermilliod and Mayor, 1989) a concentration of stars located about 0.2 mag. below the usual clump has been identified, the origin of which is still not known. This feature is also clearly seen in the clusters investigated here.

We are also accumulating orbital elements of spectroscopic binaries with red giant primaries for the analysis of their distributions and the discussion of the period-eccentricity relation. More specifically we are interested in refining the preliminary value of the limiting period for orbital circularization (Mayor and Mermilliod, 1984) and in studying the dependence of this limit on the red giant masses. Orbits for six binaries in NGC 2360 and 5822 have already been presented in Paper II (Mermilliod et al., 1989). Improved orbital elements have been obtained for NGC 2360 No. 181 and one more orbit, in IC 4756, is discussed here.

We present the observational conditions in Sect. 2 and discuss the results of the radial-velocity observations and the colour-magnitude diagram for each cluster in Sect. 3. The results on cluster mean velocity, binary frequency, and stellar evolution are discussed in Sect. 4.

2. Observations

2.1. Radial velocity

Radial-velocity observations for NGC 2423, 6811, and IC 4756 have been obtained since 1977 at the Haute-Provence Observatory (OHP) (France), with the radial-velocity scanner Coravel (Baranne et al., 1979) attached to the 1-m Swiss telescope. At least four measurements have been obtained for each star. The observations for NGC 2360 and 5822 were made from the ESO Observatory at La Silla (Chile), with the second Coravel installed on the 1.54-m Danish telescope, since 1983. At least three observations were made for each star. The radial-velocity system is the one defined by Mayor and Maurice (1985) which is a

Send offprint requests to: J.-C. Mermilliod

* Based on observations collected at the European Southern Observatory (La Silla, Chile) and at the Haute-Provence Observatory (France)

natural system for the southern Coravel. It corresponds to the IAU standard system defined by the faint list ($m_v > 4.3$). OHP observations were corrected for zero-point difference to place them in the same system. As a rule integration times were of at least three minutes for the brighter stars and up to twenty minutes for the fainter ones. Table 1 lists the names and positions of each cluster and the number of stars observed. Table A1 in the Appendix contains the 506 individual observations and gives the star identifications, Julian dates, radial velocities and internal errors, in km s^{-1}. The individual observations of the six binaries for which an orbit has already been published are not repeated here. A few new observations have been obtained.

2.2. *Photometric data*

The photometric observations were obtained during the regular campaign of observations in the stations used by the Geneva Observatory, mainly at the Gornergrat (Switzerland) and at La Silla (Chile). Data for the seven filters have been published in Rufener's (1989) fourth version of the Geneva photometric catalogue. No new photometric data in that system have been obtained for most non-member stars detected with the *RV* observations. Therefore in Tables 2, 4, 5, 6, and 7 only the *V* magnitude is given for these stars, quoted from the available *UBV* data.

3. Discussion of the clusters

3.1. *NGC 2360*

NGC 2360 is an interesting southern cluster slightly older than the Hyades. The only extensive photoelectric study was published by Eggen (1968) who derived a reddening of 0.07 mag and a corrected distance modulus of 10.3 mag from his *UBV* observations. McClure (1972) published *UBV* and DDO data for 15 red giants and derived a solar abundance for the cluster.

All 24 red giants brighter than $V = 11.5$ and redder than $B-V = 0.7$ were selected for photometric and radial-velocity observations which yielded 19 members. The results are presented in Table 1. Columns 1 and 2 give the identifications by Becker et al. (1976) and Eggen (1968), columns 3 and 4, the *V* magnitude and $[B-V]$ colour index in the Geneva system, and columns 5 to 10 present the mean radial velocity, the standard error and the number of measurements, the ratio *E/I* of the external to internal errors, the interval of time (in days) covered by the observations and the probability $P(\chi^2)$. The reader is referred to Paper I for a discussion of the instrumental errors and the definition of the probability $P(\chi^2)$ that a star is a non velocity variable. Star No. 181 is a previously unnumbered star close to the cluster center which has been identified in Paper II (Mermilliod et al., 1989). Its photometry is preliminary owing to the difficulty of separating it from the four or five close neighbours.

From the radial velocity we identify three definite non-members, stars Nos. 20, 129, and 132, the latter being variable. The membership of stars Nos. 11 and 141 is doubtful since they present radial velocity differences from the mean cluster velocity larger than 3 σ and fall outside the normal giant locus, without being binaries. All other 19 stars are considered as members. Four binaries have been discovered among the members and orbits for stars No. 51 and 181 have already been published (Mermilliod et al., 1989). We got more observations of the latter at phases between 0.8 and 1.0 which were not well covered and recomputed the orbital elements (Table 3). The radial velocity curve is not significantly modified, although the period becomes slightly longer and the amplitude slightly larger. The change of both elements produces a noticeable increase of the mass function, so that the mass ratio is close to 1. Two more stars (Nos. 68, 96) are suspected of being also binaries because $P(\chi^2)$ is smaller than 0.03.

The colour-magnitude diagram of the red giants (Fig. 1) is the first where we noticed the possible existence of the clump loop, while plotting the on-line reduced data at La Silla. Although the structure of this diagram is quite complicated, it is very reminiscent of that obtained in the composite diagram given in Paper I. According to the previous findings, the stars at $[B-V] = 0.3$ and $V < 11.2$ are identified as the real clump (core-helium burning phase). Their absolute magnitude is 0.6 according to Eggen's distance modulus, which makes sense if we adopt $M_V = 0.5$ for the Hyades-Praesepe red giants. Three to four stars fainter than $V = 11.3$ (Nos. 37, 79, 85, 134) define the fainter concentration at $[B-V] = 0.30$. Among the few stars lying within the Hertzsprung gap, one is a binary (No. 181), two are probable variables (Nos. 68 and 96), one may be a non-member (No. 141) and the last one (No. 92) seems to be normal. The binary No. 51 ($V = 11.186$,

Table 1. List of the observed clusters

Cluster	IAU	RA (1950)	Dec.	N_*[a]	Obs.
NGC 2360	C 0715−155	7 15.5	−15 32	24	ESO
NGC 2423	C 0734−137	7 34.8	−13 45	12	OHP
NGC 5822	C 1501−541	15 01.5	−54 09	28	ESO
NGC 6811	C 1936+464	19 36.7	+46 27	10	OHP
IC 4756	C 1836+054	18 36.5	+05 24	19	OHP

[a] N_* represents the number of stars observed in each cluster

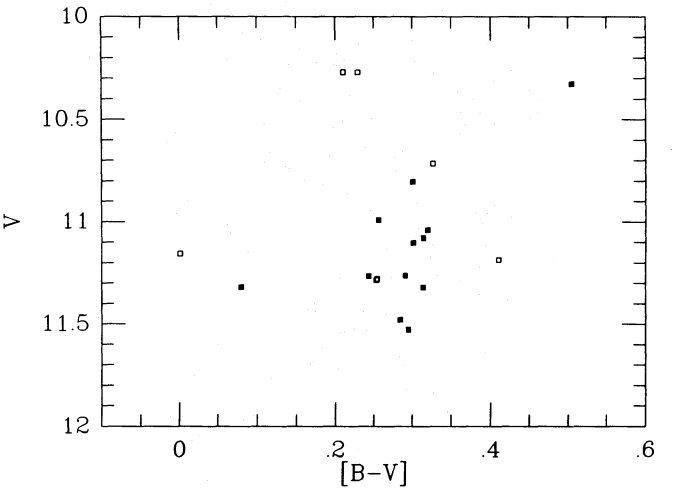

Fig. 1. Colour-magnitude diagram of the red giant members in NGC 2360. Filled squares are "single" stars and open squares represent spectroscopic binaries. With analogy with the results obtained in Paper I, the elongated clump at $[B-V] = 0.3$ is split in two parts at $V = 11.2$. The upper part ($V < 11.25$) forms the clump loop itself, while the lower part (stars nos. 37, 79, 85, 134) represents the new concentration encountered in several other clusters. See Fig. 7 for an interpretation of this diagram

Table 2. Data on NGC 2360

B	Eg	V	$[B-V]$	Vr	ε	n	E/I	ΔT	$P(\chi^2)$	Remarks
7	8	11.103	0.301	+27.18	0.25	5	1.24	2184	0.19	
37	46	11.320	0.314	+28.45	0.21	4	0.67	2199	0.74	
44	54	10.716	0.327	+20.08	0.98	12	8.78	2273	0.00	SB
50	67	11.079	0.314	+27.23	0.29	4	1.52	2199	0.08	
51	68	11.186	0.410	+27.27	0.10	26	38.43	2195	0.00	Orbit
52	69	11.280	0.254	+28.99	0.70	13	6.13	2272	0.00	SB
62	81	11.285	0.253	+27.30	0.51	4	2.23	2197	0.00	SB
66	85	11.267	0.243	+27.45	0.24	4	0.52	2182	0.85	
68		10.272	0.229	+27.32	0.27	4	1.89	2182	0.02	SB?
79	101	11.263	0.291	+27.01	0.36	4	1.70	2182	0.04	
85	109	11.480	0.284	+27.14	0.39	4	1.48	2183	0.09	
86	110	10.804	0.301	+27.29	0.28	4	1.36	2183	0.14	
89	114	10.991	0.256	+26.58	0.22	4	1.11	2198	0.30	
92	117	11.319	0.080	+26.71	0.25	4	0.86	2198	0.53	
93	118	10.328	0.505	+27.09	0.18	4	1.01	2198	0.38	
96	121	11.156	0.001	+24.74	0.50	4	1.85	2181	0.03	SB?
119	150	11.041	0.320	+27.25	0.20	4	1.00	2196	0.41	
134		11.527	0.295	+27.27	0.26	4	0.62	2196	0.77	
181		10.27	0.21	+28.13	0.19	21	15.97	1899	0.00	Orbit
11	12	11.432	0.363	+22.17	1.03	2	0.49	2184	0.64	NM?
20		11.53		+78.85	0.27	3	0.53	1811	0.75	NM
129		11.36		+54.81	0.29	4	1.14	2181	0.28	NM
132		10.94		+44.75	1.67	4	8.25	2181	0.00	NM, SB
141		10.505	0.212	+24.59	0.25	4	1.32	2181	0.17	NM?

Table 3. New orbital elements of NGC 2360–181

P	(d)	634.26	±0.48
T		5115.9	±2.1
e		0.50	±0.01
V_0	(km s^{-1})	+26.14	±0.15
ω	(deg)	211.9	±1.4
K	(km s^{-1})	22.35	±0.58
$f(m)$	($M_\odot$)	0.479	±0.050
$a \sin i$	(Gm)	1.6899	±0.0060
σ(O-C)	(km s^{-1})	0.55	

$[B-V]=0.410$) lies to the right of the clump as does star No. 92 in NGC 6940 (see Paper I).

3.2. NGC 2423

Smyth and Nandy (1962) and Hassan (1976) published *UBV* photographic data, while Eggen (1983) observed 34 stars in his *uvby-RI* system. He derived a reddening of 0.09 mag and a corrected distance-modulus of 9.8. Claria et al. (1989) obtained observations of 4 red giants in the DDO and Washington systems and determined a metal abundance similar to that of the Hyades. Twelve red giants were selected from Hassan's list, i.e. all stars redder than $B-V=0.80$ and brighter than $V=11.0$.

Table 4 presents the results. The first two columns give the identifications of Hassan (1976) and Smyth and Nandy (1962) respectively and the following ones are similar to those in Table 2. Two obvious non-members are detected (Nos. 60 and 74), the latter being a binary. All other stars are undoubtedly members. Stars Nos. 43, 70 and 235 present signs of variability. The latter (IDS 07325S1339C) is very close to the center of the cluster and to star 236 (IDS 07325S1339AB) from which it is difficult to isolate. No photometric data are available for the stars in this close system.

Although it is not very populated, the colour magnitude diagram of the red giants (Fig. 2) offers nevertheless a very clear picture of the morphology typical at these ages: four stars (Nos. 36, 43, 73, 240) fit exactly to the empirical clump curve derived in Paper I, while the brighter star (No. 15) defines an asymptotic branch slightly steeper, and hence indicating a larger age. Three stars (Nos. 20, 56, 70) are evidently located below the clump loop, the magnitude difference being 0.1 mag larger than that found for the 5 Hyades-generation clusters. Star No. 3, the second very red star is probably at the ascending branch tip. This cluster presents a good illustration of the feature we are trying to identify.

3.3. NGC 5822

This cluster is also a rather rich and interesting southern cluster which has mostly been observed in the *UBV* photographic system by Bruck et al. (1968) and Bozkurt (1974). Some photoelectric *UBV* data were found in Loden's (1979) loose clustering 2104 which corresponds to the north-west part of the cluster. Claria and Lapasset (1985) obtained new data for the red giants in the *UBV*, DDO and Washington systems, extended to more giants by Claria et al. (1989). The metal abundance is nearly solar.

Table 4. Data on NGC 2423

H	SN	*V*	[*B*−*V*]	*Vr*	ε	*n*	*E*/*I*	Δ*T*	$P(\chi^2)$	Remarks
3	4	10.066	0.594	+17.75	0.19	5	0.46	3270	0.93	
15	3	9.745	0.578	+17.74	0.16	6	0.95	3271	0.49	
20	12	11.079	0.301	+18.41	0.22	4	0.14	2971	0.99	
36	8	10.787	0.313	+17.62	0.25	5	1.21	3268	0.21	
43	5	10.435	0.344	+17.81	0.41	11	3.05	3267	0.00	SB
56	15	11.138	0.281	+18.81	0.20	8	1.16	3213	0.25	
70	14	11.101	0.287	+18.41	0.35	5	1.64	3268	0.03	SB?
73	7	10.698	0.286	+18.09	0.23	5	1.18	3267	0.23	
235				+18.79	3.02	6	10.31	2267	0.00	SB
240		10.670	0.353	+18.09	0.22	4	0.91	2268	0.48	
60	1	9.51		+29.60	0.19	5	1.03	3272	0.37	N.M.
74	21	11.40		+39.15	0.56	5	2.73	3268	0.00	N.M. SB

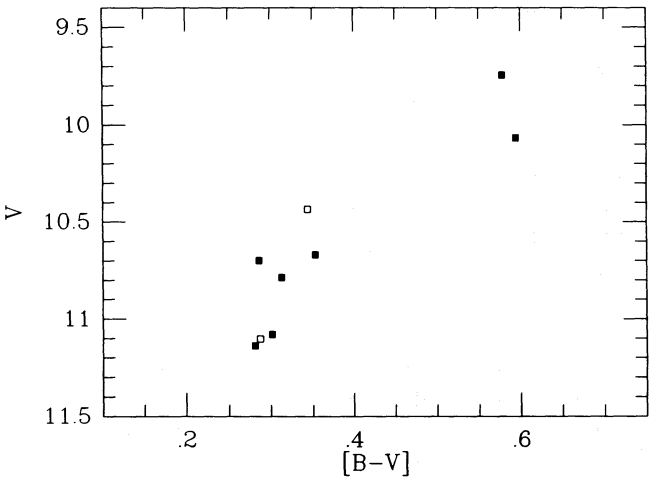

Fig. 2. Colour-magnitude diagram of the red giants in NGC 2423. Symbols are the same as in Fig. 1. Although the number of members is smaller, this diagram is very characteristic, with again a splitting of the clump. The four stars (Nos. 36, 43, 73, 240) describe the core-helium burning phase (clump), while the three stars (Nos. 20, 56, 70) 0.04 mag fainter define the second concentration. The second, fainter and redder giant may be close to the ascending branch tip. No photometric data are available for the binary giant No. 235

We selected from Bozkurt's diagram all stars with $0.7 < B-V < 1.5$ and brighter than $V = 11.8$. Star No. 148 appears too red for membership. We have used these data although they present a large scatter, because Bozkurt made the most complete investigation of the cluster area. Star No. 6 from Loden was added to the sample under No. 443. Its [*B*−*V*] colour index has been transformed from the *B*−*V* index in the Johnson system by the relation developed by Meylan and Hauck (1981).

Table 5 presents the observational results. Columns 1 and 2 give the identifications of Bozkurt (1974) and Bruck et al. (1968) respectively. The following columns are similar to those in Table 2. Seven obvious non-members were detected, this large number being due to the lower accuracy of the photometry used to define the sample. This leaves 21 members among which 8 binaries have been discovered, and two more (Nos. 4 and 271) are still suspected of variability. Both are in the position of composite binaries, are marginally variable and the mean *RV* of star 4 is slightly different from the cluster mean velocity. More observations are needed to decide upon their membership and variability. Four orbits have already been determined and published in Paper II (Mermilliod et al., 1989). The systemic velocities (V_0) are given in Table 5.

The colour-magnitude diagram of the red giants (Fig. 3) presents interesting characteristics. At about $[B-V] = 0.3$ there are two concentrations separated by 0.4 mag. They are also clearly apparent in Fig. 1 of Hirshfeld et al. (1978) based on unpublished *UBV* photographic data. In the upper one the loop is no longer apparent; it is not yet clear if the morphology is due to the presence of numerous binaries or reflects a more profound change: the shape of the clump resembles that observed in older clusters (NGC 752, M 67). The remarkable fact is the large separation between the two components and the population ratio, close to unity. Star No. 240 may be on the top of the ascending giant branch, while stars Nos. 375 and 443 are slightly on the way to the clump; star No. 1 falls on the asymptotic

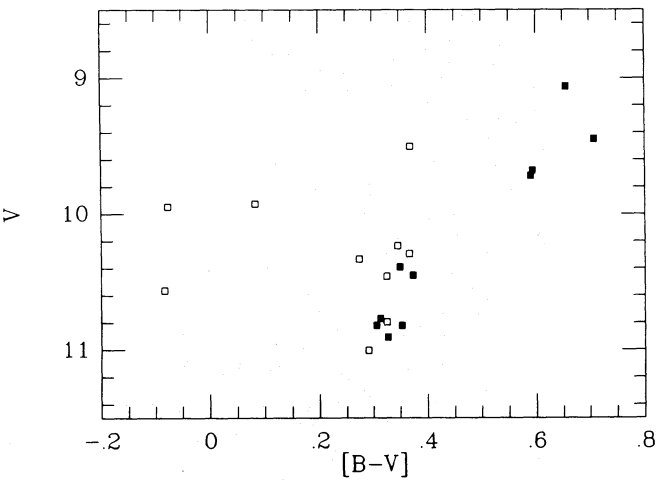

Fig. 3. Colour-magnitude diagram of red giants in NGC 5822. Symbols as in Fig. 1. Notice the large proportion of spectroscopic binaries in this cluster. The clump morcelling into two parts is here also very evident. The upper part has lost its loop structure probably because of the numerous binaries. The brighter and redder giant is on the asymptotic branch

Table 5. Data on NGC 5822

Boz	Br	V	$[B-V]$	Vr	ε	n	E/I	ΔT	$P(\chi^2)$	Remarks
1	1	9.063	0.656	−31.48	0.16	3	0.27	1468	0.93	
2	2	9.504	0.369	−29.86	1.03	12	11.49	1970	0.00	Orbit
3	3	10.293	0.367	−31.81	0.60	13	6.58	2272	0.00	SB
4	4	9.946	−0.077	−32.22	0.41	4	1.69	1069	0.05	SB?
6	6	10.770	0.313	−29.68	0.25	3	1.86	1467	0.39	
8	8	10.391	0.350	−30.92	0.22	3	0.46	1468	0.81	
11	11	11.005	0.290	−29.23	0.06	12	13.12	1970	0.00	Orbit
51		10.459	0.325	−30.65	0.58	4	3.16	1469	0.00	SB
80	58	10.330	0.273	−28.40	0.08	24	51.81	2269	0.00	Orbit
102	87	10.821	0.305	−29.82	0.28	3	1.16	1467	0.26	
151	65	10.796	0.325	−29.88	0.04	12	9.14	1970	0.00	Orbit
201	46	10.235	0.345	−28.35	0.56	3	2.57	1467	0.00	SB
224		10.821	0.353	−29.31	0.24	3	0.34	1469	0.89	
240		9.450	0.708	−29.95	0.17	3	0.56	1469	0.73	
276	149	10.565	−0.084	−29.50	0.28	8	1.50	2270	0.03	SB?
312		9.926	0.083	−31.03	1.72	15	15.26	2277	0.00	SB
316		10.455	0.374	−28.72	0.22	3	0.51	1469	0.77	
348		10.910	0.327	−29.45	0.31	3	0.72	1469	0.60	
375		9.681	0.593	−29.82	0.19	3	0.45	1468	0.82	
	157	10.938	0.336	−29.98	0.23	3	1.01	1466	0.36	
443		9.72	0.59	−29.67	0.22	4	1.64	1378	0.05	Loden No. 6
10	10	9.63		+16.60	0.17	3	0.56	1468	0.74	N.M.
148	86	10.10		−50.88	0.20	3	0.24	1468	0.94	N.M.
275	148	10.93		+10.20	0.24	3	0.83	1466	0.51	N.M.
331		11.29		−10.63	0.28	3	0.58	1469	0.71	N.M.
364		11.56		+30.92	0.39	3	0.70	1468	0.61	N.M.
387	95	11.44		−3.48	0.37	3	0.99	1467	0.39	N.M.
393	97	10.23		−15.78	0.15	6	0.48	1830	0.95	N.M.

Table 6. Data on NGC 6811

Lin	S	V	$[B-V]$	Prob.	Vr	ε	n	E/I	ΔT	$P(\chi^2)$	Remarks
24	95	11.215	0.205	0.97	+7.39	0.25	6	1.11	2951	0.32	
32	106	11.315	0.253	0.97	+6.99	0.91	5	3.90	2951	0.00	SB
101	170	10.719	0.337	0.97	+6.88	0.18	6	0.87	2951	0.61	
133	92	11.387	0.213	0.94	+7.15	0.37	5	1.38	2920	0.14	
73	64	9.89		0.00	−48.36	0.40	3	1.60	1387	0.08	N.M.
79	85	10.30		0.00	+5.12	0.21	5	1.18	2117	0.24	N.M.
210	153	9.95		0.00	−8.11	0.24	3	0.93	1387	0.43	N.M.
223	218	11.31		0.00	−39.69	0.30	3	1.03	1387	0.36	N.M.
234	186	11.10		0.96	−58.33	0.28	3	0.74	1384	0.60	N.M.
237	139	9.88		0.00	−10.54	0.25	3	0.96	1384	0.41	N.M.

branch. All stars in the lower concentration (Nos. 6, 11, 102, 151, 224, 348, Br 157) have exactly the same velocity (-29.62 ± 0.29 km s^{-1}) as the other cluster members so that their membership is very certain. This cluster offers also clear evidence for the second and fainter concentration below the clump.

3.4. NGC 6811

NGC 6811 is another Hyades-like poorly studied cluster. The only *UBV* colour-magnitude diagram published (Lindoff, 1972) presents a rather scattered main sequence from which it is difficult to determine a reliable distance modulus. The cluster is also discussed by Barkhatova et al. (1978) but the data were not published in that paper. From Lindoff's diagram all ten stars redder than $B-V=0.80$ and brighter than $V=11.5$ were selected for observations. Table 6 presents the results. Columns 1 and 2 give the identifications of Lindoff (1972) and Sanders (1971), while that headed "Prob" gives the membership probability from proper motions (Sanders, 1971). Four stars (Nos. 24, 32, 101, 133) are certainly members since the radial velocity and proper

motions results correspond well. One member is a binary. Star No. 79 could have been a long period binary member from its radial velocity, but its probability is 0.00 and it appears too red in the colour-magnitude diagram. Therefore it will not be considered in the determination of the cluster parameters. All other stars are clearly non-members. Notice also that the high membership probability from proper motion of star No. 234, which is nevertheless a non-member because of its very different radial velocity. The colour-magnitude diagram of this cluster is not presented but the four stars fall very closely on the clump loop defined by the red giants in NGC 2360.

3.5. *IC 4756*

This cluster, located at a distance of some 400 pc, has been subjected to several studies. Herzog et al. (1975) have determined membership probabilities from proper motions and produced a colour-magnitude diagram based on extensive *BV* photographic photometry. Schmidt (1978) observed red giants in the *uvby* system, and Smith (1983), in the DDO system. Both authors agreed on the presence of differential reddening in the cluster field, which complicates the analysis of the red giants in the CMD. Pendl and Seggewiss (1975) obtained 35 spectra of cluster members and determined a mean cluster velocity of $-17.2\ \mathrm{km\,s^{-1}}$.

From the *UBV* study of Alcaino (1965) and Kopff's (1943) list, 19 stars were selected. The completeness has been checked with the aid of the photographic data of Herzog et al. (1975). Table 7 collects our results. Columns 1 to 3 give the identifications of Kopff (1943), Alcaino (1965) and Herzog et al. (1975) respectively, and column 6, the membership probabilities (Herzog et al., 1975).

Two obvious non-members (Kopff, Nos. 82 and 148) have been detected, although the former has a high membership probability from the proper motions. Conversely the membership probability attributed to star No. 28 by Herzog et al. (1975) is equal to 0.0, but the radial velocity is so close to the cluster mean velocity so that it cannot be simply called a non-member. Its $[B-V]$ colour has been obtained from the $B-V$ index in the Johnson system. More debatable is the membership of star No. 48. It has a good membership probability but shows a difference of $2.8\ \mathrm{km\,s^{-1}}$ with the cluster mean velocity. Its position in the colour-magnitude diagram (Fig. 5) may be due to binarity, but, up to now, it has not shown any variability in radial velocity.

Three binaries have been discovered and one orbit determined for star No. 69. The elements are given in Table 8 and the radial velocity curve presented in Fig. 4. Although the period is long (2000 d) the eccentricity is very small: 0.04 ± 0.02. The minimum mass of the secondary is 0.54 $M_\odot$, assuming a mass of 2 $M_\odot$ for

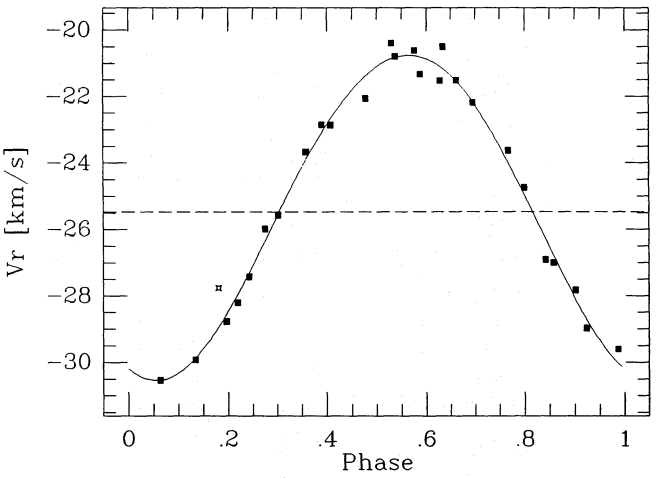

Fig. 4. Orbit of the spectroscopic binary IC 4756 No. 69. Although the period is rather long (2000 d) the eccentricity is very small (0.04). The (O−C) is equal to $0.38\ \mathrm{km\,s^{-1}}$

Table 7. Data on IC 4756

K	*A*	*H*	*V*	$[B-V]$	Prob.	*Vr*	ε	*n*	*E/I*	ΔT	$P(\chi^2)$	Remarks
12	38		9.473	0.500		−25.77	0.17	8	0.34	2570	0.99	
14	11		8.813	0.737		−25.28	0.17	7	0.74	2570	0.77	
28	16	6	8.97	0.77	0.00	−25.89	0.16	6	1.08	2541	0.33	
32	34	9	9.486	0.497	0.70	−24.39	0.16	12	1.21	3716	0.15	
38	54	35	9.756	0.416	0.82	−26.36	0.21	7	0.77	2570	0.75	
44	51	82	9.720	0.403	0.96	−26.61	0.17	9	0.81	3716	0.74	
49	31	87	9.428	0.474	0.96	−25.91	0.19	7	0.71	2570	0.80	
52	7	90	7.984	0.803	0.29	−25.87	0.14	8	0.61	2570	0.92	
69	23	144	9.201	0.366	0.96	−25.47	0.08	28	7.41	3414	0.00	Orbit
80	36	170	9.489	0.339	0.78	−29.13	0.66	32	7.82	3651	0.00	SB
81	32	176	9.362	0.354	0.91	−23.77	0.13	13	0.79	3716	0.83	M.?
101	26	228	9.362	0.354	0.94	−26.41	0.19	7	0.78	2570	0.73	
109	17	249	9.022	0.473	0.96	−25.92	0.18	7	0.85	2570	0.64	
125	27	296	9.294	0.351	0.92	−25.46	0.18	7	0.57	2570	0.93	
139	45	314	9.621	0.341	0.95	−27.01	0.32	27	3.60	3651	0.00	SB
164	24	397	9.209	0.435	0.92	−26.22	0.18	7	0.53	2570	0.95	
48	25	85	9.261	0.052	0.96	−22.53	0.17	21	1.24	3651	0.09	N.M.?
82	86	178	10.44		0.96	+32.29	0.24	5	0.88	2214	0.56	N.M.
148		350	8.97		0.00	−13.50	0.21	3	0.66	236	0.65	N.M.

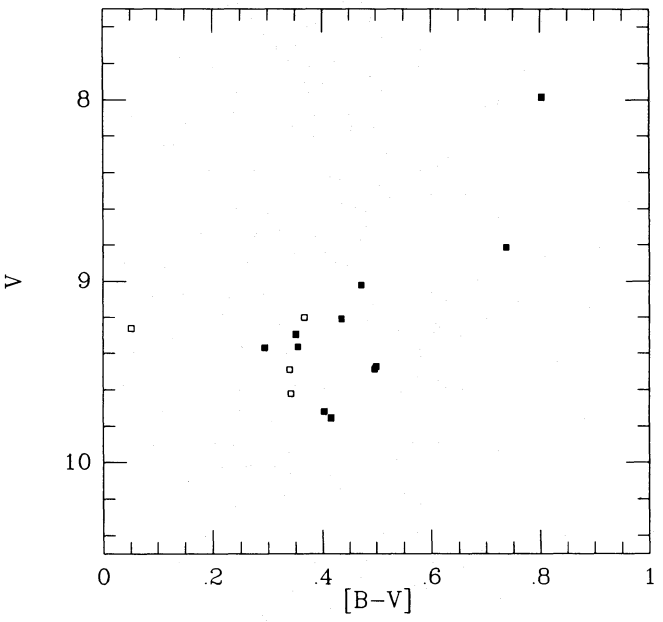

Fig. 5. Colour-magnitude diagram of the red giants in IC 4756. Symbols as in Fig. 1. The differential reddening has destroyed the evolutionary evidence

the red giant primary. The periods of the two other stars are longer than 12 yr and we have not yet covered a single entire cycle since the beginning of the observations.

The empirical isochronous curve in the colour-magnitude diagram of the red giants (Fig. 5) is completely disorganized by the effects of the differential reddening. We have tried to use the colour excesses determined by Smith (1983) from the DDO photometry, but could not rebuild a satisfactory image from these data. A more careful analysis should be done.

Table 8. Orbital elements of IC 4756–69

P	(d)	2001.0	±13.0
T		3309.0	±165.0
e		0.04	±0.02
V_0	(km s^{-1})	−25.47	±0.08
ω	(deg)	158.0	±29.0
K	(km s^{-1})	4.89	±0.12
$f(m)$	($M_\odot$)	0.0242	±0.0020
$a \sin i$	(Gm)	134.3	±4.3
σ(O−C)	(km s^{-1})	0.38	

4. Discussion

4.1. Mean cluster velocities

After selecting the cluster members, including the systemic velocities obtained from the orbits (but deleting the suspected binaries and those without an orbit) we computed the mean radial velocities for each cluster. The results are presented in Table 9, which gives in columns 1 to 4 the cluster names, the mean radial velocities, the standard errors of the mean, the dispersion of the stellar velocities and the number of stars considered.

Values for the four NGC clusters are first determinations, while that for IC 4756 differs by 8 km s^{-1} from the value published by Pendl and Seggewiss (1975). The present cluster velocity should be preferred. Eggen (1983) examined the possibility that NGC 2423 belongs to the Hyades stream because of the similarity in the ages and proper motions of the two clusters and predicted under this assumption a radial velocity equal to +35 km s^{-1}. The observed value ($Vr = +18.1$ km s^{-1}) rules out this association.

4.2. Binary frequency

Our binary detection is complete for amplitudes larger than 4.0 km s^{-1} or periods smaller than 4000 d, since most observations were made over an interval of more than 2000 d. The probability $P(\chi^2)$ shows few ambiguous cases: seven stars among the 71 members have non-zero values of $P(\chi^2)$ less or equal to 0.05. Corrected for false detection, we still have an excess of 3 to 4 probable binaries. The overall binary frequency is 27%, namely 19 binaries among 71 red giant members and reaches 32% if 4 suspected binaries are included. Table 9 (columns 6 to 9) presents the figures: the number of members, of detected binaries, of suspected binaries and the expected numbers computed with the mean percentage. There is a very good agreement between the computed and observed values. The binary frequency of the clump stars and those in the fainter concentration are very similar.

4.3. Stellar evolution

Except for NGC 2360 observed photoelectrically by Eggen (1968), accurate distance moduli for the clusters investigated here cannot be determined because photoelectric data are too scanty to define precisely the main-sequence and turn-off. The numerous

Table 9. Results

Cluster	Vr	ε (km s^{-1})	σ	n	N_m	N_{SB}	$N_{SB?}$	N_c
NGC 2360	+27.24	0.13	0.45	12	20	5	2	5.40
NGC 2423	+18.07	0.16	0.42	7	10	2	1	2.70
NGC 5822	−29.74	0.19	0.75	15	21	8	2	5.67
NGC 6811	+7.14	0.15	0.26	3	4	1	0	1.08
IC 4756	−25.81	0.16	0.58	13	16	3	0	4.32
Total (5 clusters)					71	19	5	

photographic data in the *UBV* system do not help at all because the data for NGC 5822 (Bozkurt, 1974) and 6811 (Lindoff, 1972) are too imprecise and those for NGC 2423 and 2360 contain systematic errors: the *V* magnitude of Hassan (1976) in NGC 2423 is wrong by 0.7 mag and Becker et al.'s (1976) data in NGC 2360 show systematic trends in function of the colour. In addition IC 4756 presents differential reddening. It is therefore not possible to derive absolute parameters from the main sequence fitting as accurate as needed for a relative location of the red giant sequences. Modern photometric data of these clusters and in general of most objects older than the Hyades would be very helpful.

As can be judged from the magnitude difference between the clump loop and the top of the main sequence, all clusters are slightly older than the Hyades. The isochrone computed from Maeder and Meynet (1989) models with core overshooting and mass loss and fitted to Eggen's (1968) *UBV* photoelectric data in NGC 2360 (Fig. 6) suggests an age close to 2.2 10^9 yr ($\log t = 9.35$). (The age obtained for Praesepe from the same grid of models is $\log t = 9.20$.) The isochrone reproduces fairly well the extension of the main sequence, but the red giant branch appears too red, in spite of the care taken in the models to obtain a good match. This difference is probably due to the value of the mixing length parameter (1.9) chosen here (Maeder, 1990). Maeder and Meynet (1989) discussed the choice of this value and the implication of other choices are shown in their Fig. 2. As seen in Fig. 6, no direct comparison can be made between the observed red giant distribution in the CM diagram and the isochrone without applying some corrections to the theoretical track.

In an effort to understand the distribution of the red giants in the colour-magnitude diagrams, we have computed an isochrone with core overshooting for the same age ($\log t = 9.35$) in the Geneva $[B-V]$ colour and shifted it horizontally to correct for the effect noticed in Fig. 6. With a second upwards shift of 0.1 mag, (which may be justified by a change on the bolometric correction due to the change in effective temperature) we obtained a surprisingly good fit to the observations (Fig. 7). Seven stars (black square) and one binary (open square) describe well the clump loop. Two stars (Nos. 68 and 96), bluer than $[B-V] = 0.10$ are suspected binaries. There are three (and may be four) points below the isochrone. Their existence may be justified by the reason already advanced in Paper I: the encounter of the H-burning shell advancing outwards with major hydrogen-abundance discontinuities should produce a slow down in the ascension of the giant branch resulting in an excess number of red giants in the clump region (Demarque and Heasley, 1971). These three stars, and those noticed in the colour-magnitude diagram of NGC 2423 (Fig. 8) in which the same isochrone has been plotted, could be explained by this feature. According to Maeder and Meynet (1989) this phenomenon occurs however in stars less massive than 1.7 $M_\odot$, while our stars are slightly more massive. Finally the slope of the asymptotic branch is slightly too steep and the most evolved stars cannot be attributed to the giant branch tip or asymptotic branch with certainty, although the latter solution seems preferable.

This comparison is not really a fit of a model to observations, but has been done as an attempt to understand the complex structure of the red giant track. It seems to have been quite successful and it is hoped that the models will be improved so that the isochrones could match at the same time the main sequence and the red giant branch. It shows at least that with a good

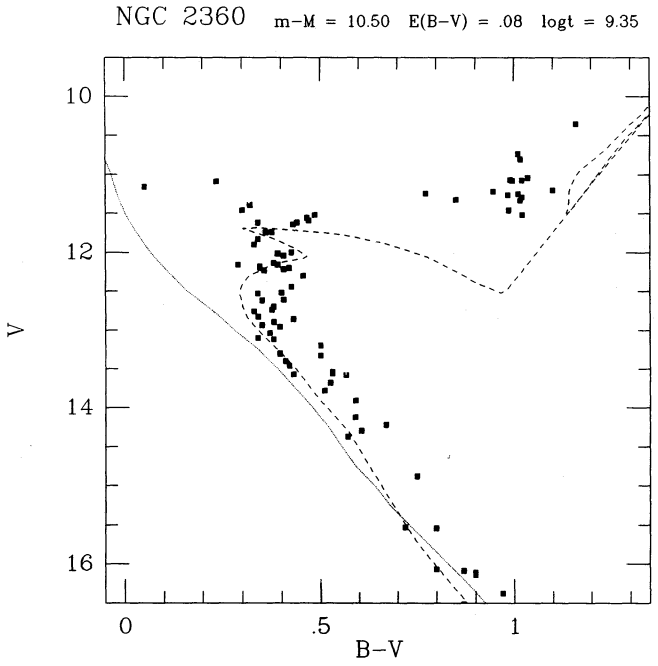

Fig. 6. Colour-magnitude diagram of NGC 2360 from Eggen's (1968) *UBV* data. The isochrone computed from Maeder and Meynet's (1989) models with core overshooting corresponds to an age of 2.2 10^9 yr

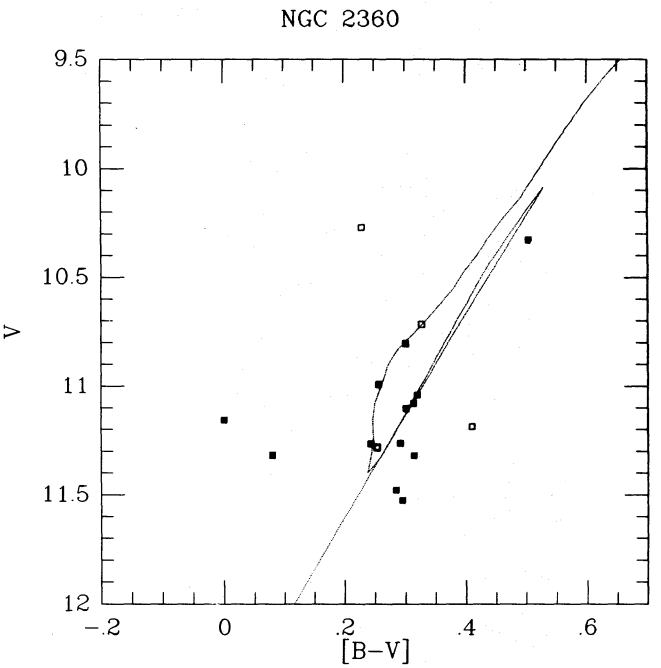

Fig. 7. Colour-magnitude diagram of the red giants in NGC 2360 with an isochrone ($\log t = 9.35$) with core overshooting. In spite of the slightly too steep slope of the asymptotic branch, the fit is quite convincing and helps in understanding the evolutionary status of each red giant. The width of the loop is much larger than the photometric errors, both in colour and magnitude. The three stars well below the isochrone, referred to as the second and fainter star concentration in Paper I, could be explained by the process described by Demarque and Heasley (1971)

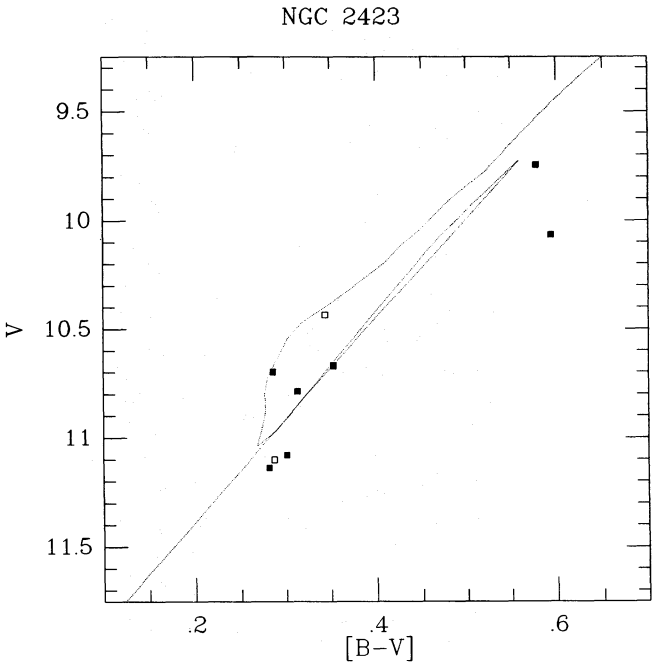

Fig. 8. Same diagram as in Fig. 7, but for NGC 2423. The isochrone has the same age as before and provides also a good description of the red giant distribution in that plane

knowledge of the non-binary members and precise photometry it is possible to define experimentally the evolutionary path during the red giant phase. Results on intermediate-age open clusters containing more red giants will be very important in that respect.

Assuming that the ages of the present clusters are comprised between $\log t = 9.3$ and 9.4, the masses of the stars at the end of the hydrogen-burning phase are between 1.9 and 1.8 $M_\odot$ respectively. Therefore, these clusters offer the first direct observational evidence of the effects of overshooting on the red giant colour-magnitude diagram, in agreement with the finding of Barbaro and Pigatto (1984) and the theoretical prediction of Maeder and Meynet (1989). As shown by Figs. 6 and 7, they do not present the long giant branch predicted by standard models (without overshooting), but behave instead like younger clusters (with turn-off masses larger than 2.2 $M_\odot$). Our results, which are independent of the problems in the position of the theoretical giant branch, confirm that the limiting mass for helium flash is smaller than 2.2 $M_\odot$. The exact value will be further constrained by the analysis of still older clusters, like NGC 752, 3680 and IC 4651 which will be discussed in a subsequent paper.

No composite diagram has been formed for these five clusters because the age differences do not allow an exact superposition of the red giant sequences.

5. Conclusion

Radial velocity observations of 93 red giants in five open clusters older than the Hyades allowed the selection of 71 members and the discovery of 19 spectroscopic binaries. One new orbit, for IC 4756 No. 69, has been determined in addition to the six published in Paper II. The binary percentage of this sample is equal to 27%, or to 32% if the probable binaries are taken into account. Many fewer composite binaries have been found than in Paper I. Only two among the 22 non-member stars detected are spectroscopic binaries.

The photometric data in the Geneva system of the red giants produce the same kind of colour-magnitude diagrams. The clump is split in two sub-concentrations separated by 0.2 to 0.4 mag, this value being larger in the older cluster (NGC 5822). The number ratio between both concentrations is close to unity in NGC 5822. The membership of the stars in the fainter concentration cannot be rejected because their radial velocities are exactly the same as those of the other members. This feature is also not an artefact of the Geneva photometry measurements since it is very well apparent in the colour-magnitude diagram for NGC 5822 published by Hirshfeld et al. (1978). Our interpretation is supported by the comparison of isochrones with core overshooting and the observed colour-magnitude diagram.

In addition the overall morphology of the colour-magnitude diagrams for these red giants with mass smaller than 2.0 $M_\odot$, in which the clump is the main feature, brings support to the models with core overshooting against the standard models which predict a long giant branch as observed in M 67. This implies that the limiting mass for helium flash must be smaller than 2.2 $M_\odot$.

Acknowledgements. We are grateful to A. Maeder and M. Meynet for the permission to use their program for computing the isochrones. This work has been supported by continuous grants from the Swiss National Foundation for Scientific Research (FNRS). We also thank ESO for telescope-time allotment.

References

Alcaino, G.: 1965, *Lowell Obs. Bull. VI* no. **126**
Baranne, A., Mayor, M., Poncet, J.-L.: 1979, *Vistas Astron.* **23**, 279
Barbaro, G., Pigatto, L.: 1984, *Astron. Astrophys.* **136**, 355
Barkhatova, K.A., Zakharova, P.E., Shashkina, L.P.: 1978, *Sov. Astron.* **22**, 31
Becker, W., Svolopoulos, S.N., Fang, C.: 1976, *Katalog photographischer und photoelektrischer Helligkeiten von 25 galaktischen Sternhaufen im RGU-und U_cBV-System* Univ. Basel
Bozkurt, S.: 1974, *Rev. Mex. Astron. Astrofis.* **1**, 89
Bruck, M.T., Smyth, M.J., McLachlan, A.:1968, *Publ. R. Obs. Ed.* **6**, 209
Claria, J.J., Lapasset, E.: 1985, *Monthly Notices Roy. Astron. Soc.* **214**, 229
Claria, J.J., Lapasset, E., Minniti, D.: 1989, *Astron. Astrophys. Suppl.* **78**, 363
Demarque, P., Heasley, J.N.: 1971, *Monthly Notices Roy. Astron. Soc.* **155**, 85
Eggen, O.J.: 1968, *Astrophys. J.* **152**, 83
Eggen, O.J.: 1983, *Astron. J.* **88**, 190
Eggen, O.J.: 1987, *Astron. J.* **88**, 190
Hassan, S.M.: 1976, *Astron. Astrophys. Suppl.* **26**, 13
Herzog, A.D., Sanders, W.L., Seggewiss, W.: 1975, *Astron. Astrophys. Suppl.* **19**, 211
Hirshfeld, A., McClure, R.D., Twarog, B.A.: 1978, in *The HR diagram*, eds. A.G.D. Philip, D.S. Hayes, p. 163
Kopff, E.: 1943, *Astron. Nach.* **274** no. 2
Lindoff, U.: 1972, *Astron. Astrophys.* **16**, 315
Loden, L.O.: 1979, *Astron. Astrophys. Suppl.* **38**, 355
Maeder, A.: 1990, private communication
Maeder, A., Meynet, G.: 1989, *Astron. Astrophys.* **210**, 155

Appendix: Table A1

NGC 2360 # 7

5389.569	+27.0	0.4
5762.582	+27.9	0.4
6469.548	+26.5	0.5
6869.504	+27.2	0.5
7573.646	+26.8	0.4

NGC 2360 # 11

5389.574	+21.1	2.6
7573.659	+22.4	1.2

NGC 2360 # 20

5762.573	+79.1	0.4
6468.594	+78.8	0.5
7573.642	+78.6	0.5

NGC 2360 # 37

5389.589	+29.1	0.6
5762.567	+28.4	0.4
6469.551	+28.5	0.6
7588.566	+28.3	0.3

NGC 2360 # 44

5389.594	+27.4	0.5
5762.563	+26.6	0.4
6469.554	+19.2	0.5
6470.625	+19.4	0.4
6523.538	+19.1	0.3
6748.804	+18.2	0.5
6812.706	+16.4	0.3
6863.545	+16.9	0.5
7189.664	+18.8	0.3
7509.563	+22.1	0.5
7573.621	+22.2	0.5
7662.465	+22.2	0.4

NGC 2360 # 50

5389.598	+27.7	0.4
5762.560	+27.8	0.4
6469.557	+27.4	0.5
7588.573	+26.7	0.3

NGC 2360 # 51

Orbit in paper II

7585.524	+50.8	0.4

NGC 2360 # 52

5390.572	+23.2	0.5
5760.598	+24.1	0.4
6469.562	+27.8	0.5
6523.531	+28.2	0.3
6748.797	+29.9	0.5
6812.715	+29.3	0.3
6850.367	+29.6	0.6
6863.539	+29.3	0.5
7189.671	+31.1	0.3
7206.407	+31.1	0.5
7509.569	+31.1	0.6
7573.626	+31.3	0.4
7662.471	+30.8	0.4

NGC 2360 # 62

5391.501	+27.7	0.6
5760.562	+27.7	0.4
6470.614	+28.4	0.5
7588.580	+26.1	0.4

NGC 2360 # 66

5391.505	+27.1	0.6
5760.557	+27.4	0.5
6470.616	+27.6	0.5
7573.673	+27.6	0.4

NGC 2360 # 68

5391.508	+26.8	0.3
5760.551	+27.8	0.2
6470.619	+27.5	0.3
7573.677	+26.7	0.3

NGC 2360 # 79

5391.511	+27.5	0.5
5760.568	+27.0	0.4
6470.622	+28.1	0.6
7573.681	+26.2	0.4

NGC 2360 # 85

5390.590	+27.2	0.5
5760.582	+26.2	0.5
6469.577	+27.8	0.6
7573.612	+27.8	0.6

NGC 2360 # 86

5390.587	+28.2	0.5
5760.577	+27.1	0.3
6469.574	+26.7	0.5
7573.608	+27.2	0.4

NGC 2360 # 89

5390.576	+27.2	0.4
5760.592	+26.5	0.4
6469.565	+26.3	0.5
7588.586	+26.3	0.3

NGC 2360 # 92

5390.580	+26.7	0.5
5760.506	+27.1	0.5
6469.568	+27.0	0.6
7588.592	+26.2	0.4

NGC 2360 # 93

5390.583	+27.3	0.3
5760.573	+26.6	0.3
6469.571	+27.1	0.4
7588.596	+27.4	0.3

NGC 2360 # 96

5392.505	+25.2	1.0
5760.604	+25.4	0.4
6469.580	+25.3	0.8
7573.617	+23.4	0.5

NGC 2360 # 119

5392.514	+27.9	0.6
5763.557	+27.4	0.4
6469.583	+27.4	0.5
7588.601	+26.9	0.3

NGC 2360 # 129

5392.552	+55.6	0.6
5763.572	+54.5	0.4
6470.633	+55.4	0.6
7573.635	+54.4	0.5

NGC 2360 # 132

5392.544	+47.8	0.5
5763.564	+46.6	0.3
6470.630	+45.3	0.4
7573.631	+40.1	0.4

NGC 2360 # 134

5392.539	+27.7	0.6
5763.561	+27.1	0.5
6470.628	+27.6	0.7
7588.606	+27.1	0.5

NGC 2360 # 141

5392.556	+24.6	0.6
5763.568	+24.1	0.3
6470.636	+25.1	0.4
7573.639	+24.9	0.4

NGC 2360 # 181

Orbit in paper II

7505.635	+22.5	0.8
7548.640	+14.4	0.8
7554.437	+14.9	0.6
7573.604	+9.1	0.7
7662.478	+2.4	0.6

NGC 2423 # 3

4284.394	+17.5	0.5
4583.632	+18.1	0.5
5285.661	+17.7	0.4
6420.568	+17.7	0.4
7554.446	+17.8	0.4

NGC 2423 # 15

4283.455	+17.2	0.5
4583.648	+18.2	0.5
5032.329	+18.1	0.4
5285.656	+17.4	0.4
6420.578	+18.0	0.4
7554.451	+17.4	0.4

NGC 2423 # 20

4583.640	+18.4	0.5
5356.498	+18.5	0.4
6440.477	+18.4	0.6
7554.458	+18.3	0.4

NGC 2423 # 36

4287.432	+17.6	0.5
4583.623	+18.0	0.5
5356.532	+18.3	0.5
6440.486	+16.9	0.6
7555.433	+17.2	0.4

NGC 2423 # 43

4287.367	+18.9	0.5
4583.669	+20.2	0.5
5052.310	+16.7	0.6
5285.648	+17.2	0.4
5673.618	+18.6	0.4
6440.492	+19.3	0.5
6766.620	+15.7	0.5
6820.454	+16.3	0.4
7118.657	+16.8	0.4
7510.547	+18.9	0.5
7554.485	+17.8	0.4

NGC 2423 # 56

4341.324	+17.9	1.0
4583.658	+18.3	0.5
5356.518	+18.9	0.4
5673.612	+19.3	0.4
6440.502	+19.3	0.5
6766.612	+19.8	0.6
7118.667	+18.3	0.4
7554.468	+18.5	0.5

NGC 2423 # 60

4283.444	+29.7	0.5
4583.582	+30.4	0.5
5356.482	+29.2	0.4
6420.587	+29.5	0.4
7555.427	+29.4	0.4

NGC 2423 # 70

4287.423	+18.0	0.5
4583.590	+18.9	0.5
5356.548	+19.5	0.5
6442.511	+17.8	0.5
7555.441	+17.8	0.4

NGC 2423 # 73

4287.384	+18.0	0.5
4583.599	+18.8	0.5
5285.668	+18.0	0.4
6442.520	+18.5	0.4
7554.495	+17.4	0.4

NGC 2423 # 74

4287.406	+38.4	0.6
4583.611	+38.4	0.5
5370.463	+37.8	0.5
6442.528	+39.1	0.5
7555.452	+40.9	0.4

NGC 2423 # 235

5287.661	+10.9	0.8
6442.553	+17.1	0.6
6766.628	+25.1	0.9
7118.679	+13.9	0.7
7206.438	+16.7	0.8
7554.478	+30.6	0.7

NGC 2423 # 240

5287.640	+18.6	0.4
5356.565	+17.7	0.5
6420.595	+17.9	0.5
7555.422	+18.1	0.4

NGC 5822 # 1

5397.842	-31.5	0.4
5760.869	-31.5	0.3
6865.854	-31.4	0.2

NGC 5822 # 2

Orbit in paper II

NGC 5822 # 3

5397.893	-26.4	0.5
5760.863	-29.3	0.3
5875.569	-30.5	0.6
6160.781	-32.7	0.3
6291.505	-33.9	0.3
6468.865	-34.0	0.3
6645.487	-33.5	0.4
6669.522	-33.9	0.3
6862.840	-32.9	0.4
6973.589	-31.7	0.4
7229.866	-31.8	0.3
7367.565	-30.3	0.3
7669.723	-28.7	0.3

NGC 5822 # 4

5398.836	-31.6	0.5
5760.859	-33.4	0.5
5877.651	-32.5	1.0
6467.882	-31.8	0.4

NGC 5822 # 6

5398.841	-29.4	0.5
5760.866	-30.1	0.4
6865.859	-29.4	0.4

NGC 5822 # 8

5397.848	-31.2	0.5
5761.877	-30.8	0.3
6865.863	-30.9	0.4

NGC 5822 # 10

5397.859	+16.7	0.4
5761.869	+16.7	0.3
6865.867	+16.4	0.3

NGC 5822 # 11

Orbit in paper II

NGC 5822 # 51

5398.847	-32.0	0.4
5761.845	-29.2	0.4
6468.868	-30.4	0.4
6867.842	-30.9	0.4

NGC 5822 # 80

Orbit in paper II

7666.771	-42.4	0.3

NGC 5822 # 102

5398.886	-29.5	0.4
5760.872	-29.5	0.4
6865.891	-30.4	0.4

NGC 5822 # 148

5397.881	-50.9	0.5
5761.860	-50.8	0.3
6865.871	-51.0	0.3

NGC 5822 # 151

Orbit in paper II

NGC 5822 # 201

5398.891	-27.9	0.4
5762.844	-27.6	0.4
6865.895	-29.3	0.3

NGC 5822 # 224

5398.881	-29.2	0.4
5760.880	-29.2	0.5
6867.846	-29.5	0.4

Table A1 (continued)

NGC 5822 # 240

5398.851	-30.0	0.3
5760.888	-30.1	0.3
6867.850	-29.8	0.3

NGC 5822 # 275

5399.846	+9.7	0.5
5761.853	+10.4	0.4
6865.881	+10.2	0.4

NGC 5822 # 276

5399.852	-28.4	0.8
5761.856	-28.9	0.6
6467.886	-29.3	0.6
6865.877	-29.8	0.5
6973.578	-28.3	0.6
7229.853	-30.1	0.4
7367.600	-29.1	0.5
7669.727	-30.8	0.5

NGC 5822 # 312

5398.856	-27.2	0.6
5761.834	-33.7	0.5
5877.686	-40.5	1.1
6160.800	-23.9	0.4
6290.498	-25.0	0.4
6468.871	-27.0	0.6
6645.519	-31.6	0.5
6667.499	-31.8	0.5
6862.845	-42.4	0.5
6973.584	-51.1	0.5
7229.858	-24.7	0.5
7367.557	-26.8	0.4
7574.883	-30.8	0.3
7669.719	-33.0	0.4
7675.694	-33.1	0.4

NGC 5822 # 316

5398.861	-28.9	0.4
5761.837	-28.5	0.4
6867.853	-28.8	0.4

NGC 5822 # 331

5398.868	-10.6	0.5
5761.841	-10.3	0.5
6867.858	-10.9	0.5

NGC 5822 # 348

5398.874	-29.5	0.4
5760.883	-29.7	0.4
6867.863	-29.1	0.5

NGC 5822 # 364

5399.868	+30.4	0.7
5762.856	+31.2	0.6
6867.870	+31.2	0.8

NGC 5822 # 375

5399.873	-29.9	0.4
5762.854	-29.9	0.3
6867.874	-29.6	0.4

NGC 5822 # 387

5398.898	-4.0	0.8
5762.847	-2.9	0.6
6865.899	-3.9	0.7

NGC 5822 # 393

5399.877	-16.0	0.5
5762.850	-15.9	0.3
6645.527	-15.5	0.3
6865.903	-15.9	0.4
6973.596	-15.8	0.4
7229.871	-15.7	0.3

NGC 5822 # 443

6291.492	-30.3	0.3
6645.543	-29.5	0.3
7229.876	-29.5	0.3
7669.731	-29.4	0.2

NGC 5822 #1157

5399.858	-30.4	0.5
5761.849	-29.6	0.4
6865.886	-30.1	0.3

NGC 6811 # 24

3698.499	+6.7	0.6
3729.428	+8.5	1.1
4076.514	+7.7	0.6
4485.450	+8.3	0.7
5580.398	+7.5	0.4
6649.433	+6.9	0.5

NGC 6811 # 32

3698.509	+3.1	0.7
4078.458	+8.2	0.7
4846.390	+7.7	0.6
5580.407	+6.0	0.4
6649.442	+8.7	0.4

NGC 6811 # 73

4880.312	-48.7	0.4
5170.473	-48.6	0.4
6267.441	-47.3	0.5

NGC 6811 # 79

4880.319	+4.6	0.4
5170.482	+5.3	0.4
5580.389	+5.8	0.4
5915.501	+4.8	0.4
6997.506	+5.1	0.5

NGC 6811 # 101

3698.528	+7.1	0.5
4078.480	+6.7	0.5
4485.408	+6.2	0.6
4581.233	+7.3	0.5
5580.381	+7.2	0.4
6649.472	+6.7	0.3

NGC 6811 # 133

3729.438	+8.4	1.4
4078.501	+6.9	0.7
4846.396	+8.1	0.6
5580.426	+7.3	0.5
6649.451	+6.1	0.6

NGC 6811 # 210

4880.326	-8.3	0.4
5170.499	-8.2	0.4
6267.446	-7.5	0.5

NGC 6811 # 223

4880.336	-40.1	0.4
5287.285	-39.2	0.5
6267.451	-39.5	0.7

NGC 6811 # 234

4883.285	-58.0	0.4
5170.460	-58.6	0.4
6267.461	-58.3	0.8

NGC 6811 # 237

4883.275	-10.2	0.4
5170.449	-10.7	0.4
6267.456	-11.0	0.6

IC 4756 # 12

3701.440	-26.0	0.5
3788.316	-25.5	0.5
4027.568	-25.7	0.7
4095.379	-25.8	0.5
4384.605	-25.6	0.5
4463.441	-25.8	0.5
5159.513	-25.9	0.5
6271.506	-25.7	0.5

IC 4756 # 14

3701.434	-25.4	0.5
3788.326	-25.7	0.5
4027.564	-25.7	0.5
4090.405	-25.3	0.4
4384.601	-25.2	0.5
5159.518	-25.2	0.4
6271.502	-24.7	0.4

IC 4756 # 28

4876.277	-25.7	0.4
4885.280	-25.8	0.4
5027.684	-26.0	0.4
5159.502	-25.8	0.4
5915.375	-26.6	0.3
7417.305	-25.4	0.4

IC 4756 # 32

3701.444	-24.3	0.5
3788.335	-23.9	0.5
4027.556	-24.4	0.7
4095.388	-24.1	0.5
4384.609	-24.4	0.5
4463.448	-24.2	0.5
4876.291	-23.6	0.4
5050.677	-24.4	0.4
5159.507	-24.8	0.5
5524.483	-24.5	0.4
5915.381	-25.6	0.4
7417.312	-24.3	0.4

IC 4756 # 38

3701.448	-26.2	0.5
3747.434	-26.9	0.7
4027.551	-26.1	0.6
4095.398	-26.1	0.5
4396.587	-27.1	0.6
5169.436	-26.0	0.5
6271.499	-26.6	0.6

IC 4756 # 44

3701.453	-27.3	0.6
3788.343	-26.1	0.5
4025.603	-26.1	0.7
4095.412	-26.9	0.5
4384.614	-26.5	0.6
5050.683	-27.0	0.4
5159.496	-26.5	0.5
6271.494	-26.8	0.6
7417.320	-26.3	0.4

IC 4756 # 48

3701.463	-22.6	0.7
3747.414	-21.0	1.0
4025.592	-22.9	0.8
4090.413	-21.2	0.6
4099.391	-22.2	0.7
4107.394	-21.7	1.3
4287.723	-23.7	0.7
4384.624	-22.1	0.9
4401.542	-23.0	0.6
4463.433	-23.9	0.7
4486.420	-22.7	0.4
4846.351	-21.9	0.7
4876.301	-22.4	0.7
4877.281	-21.8	0.7
4878.279	-22.2	0.5
4885.286	-21.5	0.7
5159.485	-23.2	0.8
5915.387	-23.6	0.6
6271.490	-21.9	0.8
6911.646	-22.4	0.6
7352.478	-23.5	0.7

IC 4756 # 49

3701.469	-25.9	0.5
3747.397	-26.0	0.6
4025.582	-25.5	0.5
4095.423	-26.0	0.5
4396.581	-26.2	0.6
5159.480	-25.4	0.5
6271.481	-26.4	0.4

IC 4756 # 52

3701.456	-25.7	0.5
3747.405	-25.9	0.5
4025.597	-25.6	0.4
4089.442	-25.6	0.4
4384.620	-25.6	0.4
5050.670	-26.2	0.3
5159.490	-26.0	0.3
6271.485	-26.1	0.3

IC 4756 # 69

3701.475	-28.8	0.5
3747.373	-28.2	0.6
4025.571	-23.7	0.5
4090.422	-22.9	0.5
4384.631	-20.8	0.5
4463.427	-20.6	0.5
4486.435	-21.3	0.5
4566.262	-21.5	0.5
4634.718	-21.5	0.5
4846.357	-23.6	0.4
5027.690	-27.0	0.4
5159.471	-29.0	0.4
5285.281	-29.6	0.4
5437.626	-30.5	0.5
5578.338	-29.9	0.4
5672.219	-27.8	0.4
5797.605	-27.4	0.4
5861.597	-26.0	0.4
5915.393	-25.6	0.4
6030.250	-23.7	0.5
6127.659	-22.9	0.5
6267.397	-22.1	0.4
6372.231	-20.4	0.4
6580.590	-20.5	0.6
6704.302	-22.2	0.4
6911.631	-24.8	0.5
6995.478	-26.9	0.4
7115.245	-27.8	0.4

IC 4756 # 80

3701.490	-24.4	0.5
3747.389	-23.0	0.8
4025.551	-26.4	0.5
4090.429	-27.5	0.5
4107.408	-27.1	0.7
4396.567	-29.2	0.6
4463.455	-30.9	0.6
4486.440	-30.6	0.5
4566.273	-29.7	0.6
4846.363	-31.8	0.5
4877.293	-31.4	0.4
5027.695	-32.9	0.4
5159.524	-33.2	0.5
5285.287	-32.9	0.5
5437.635	-33.8	0.6
5578.343	-32.8	0.5
5672.224	-32.0	0.4
5797.614	-32.4	0.4
5861.593	-32.5	0.4
5915.399	-32.4	0.5
6032.216	-31.4	0.4
6127.665	-31.0	0.6
6267.403	-30.4	0.5
6372.236	-29.5	0.5
6580.593	-27.9	0.6
6643.481	-27.7	0.5
6704.306	-26.7	0.4
6911.636	-23.8	0.5
6995.485	-24.7	0.4
7115.251	-23.7	0.5
7245.678	-22.1	0.5
7352.468	-21.8	0.4

IC 4756 # 81

3701.480	-23.8	0.5
3747.380	-24.0	0.6
4025.565	-23.8	0.5
4090.437	-24.0	0.5
4396.562	-23.7	0.6
4486.447	-23.9	0.6
4877.287	-23.2	0.4
5050.689	-23.5	0.5
5159.475	-23.6	0.5
5524.489	-24.4	0.4
5861.588	-23.2	0.4
6271.477	-23.9	0.5
7417.328	-24.1	0.4

Table A1 (continued)

IC 4756 # 82			IC 4756 # 109(cont.)			IC 4756 # 139(cont.)			IC 4756 # 148		
3701.485	+32.5	0.5	4396.535	-26.6	0.5				5561.363	-13.8	0.3
3702.471	+31.6	0.6	5159.451	-26.3	0.5	4846.369	-27.5	0.4	5584.316	-13.5	0.4
4025.558	+31.8	0.6	6271.469	-25.6	0.4	5027.702	-28.4	0.4	5797.630	-13.3	0.3
4396.574	+32.5	0.8				5159.447	-28.2	0.5	5561.363	-13.8	0.3
5915.406	+32.7	0.4	IC 4756 # 125			5285.276	-28.1	0.5	5584.316	-13.5	0.4
						5437.619	-28.5	0.5	5797.630	-13.3	0.3
IC 4756 # 101			3701.505	-26.0	0.5	5578.350	-28.6	0.4	5561.363	-13.8	0.3
			3746.436	-25.6	0.6	5672.233	-27.5	0.4	5584.316	-13.5	0.4
3701.495	-26.4	0.5	4025.519	-25.2	0.5	5797.622	-29.1	0.4	5797.630	-13.3	0.3
3747.356	-25.7	0.6	4092.408	-25.2	0.5	5861.581	-27.8	0.5			
4025.544	-25.9	0.5	4396.547	-25.3	0.5	5915.415	-29.1	0.4			
4098.409	-26.4	0.5	5159.441	-25.5	0.5	6030.261	-27.9	0.7			
4396.540	-26.6	0.5	6271.461	-25.5	0.4	6127.671	-28.5	0.6			
5159.456	-26.6	0.5				6267.413	-28.3	0.5	IC 4756 # 164		
6271.473	-26.9	0.5	IC 4756 # 139			6372.241	-26.8	0.5			
						6580.596	-27.8	0.7	3701.515	-25.9	0.5
IC 4756 # 109			3701.511	-24.2	0.5	6704.309	-27.4	0.4	3746.456	-26.0	0.7
			3746.446	-23.7	0.7	6911.641	-25.8	0.5	4025.525	-26.5	0.5
3701.499	-25.8	0.5	4025.531	-23.8	0.5	6995.492	-26.1	0.4	4092.415	-26.3	0.5
3747.366	-25.6	0.6	4098.418	-23.8	0.5	7115.256	-25.6	0.4	4396.551	-26.2	0.5
4025.538	-25.6	0.5	4396.556	-25.3	0.6	7245.682	-25.2	0.4	5159.529	-26.0	0.5
4090.449	-25.9	0.5	4463.461	-26.2	0.5	7352.473	-25.3	0.5	6271.465	-26.4	0.4

Mayor, M., Maurice, E.: 1985, *IAU Coll.* no. **88**, eds. A.G.D. Philip, D.W. Latham, L. Davis Press, Schenectady, N.Y., p. 35

Mayor, M., Mermilliod, J.-C.: 1984, *Observational Tests of the Stellar Evolution Theory*, *IAU Symp.* no. **105**, eds. A. Maeder, A. Renzini, Reidel, Dordrecht, p. 411

McClure, R.D.: 1972, *Astrophys. J.* **172**, 622

Mermilliod, J.-C., Mayor, M.: 1989, *Astron. Astrophys.* **219**, 125

Mermilliod, J.-C., Mayor, M., Andersen, J., Nordstrom, B., Lingren, H., Duquennoy, A.: 1989, *Astron. Astrophys. Suppl.* **79**, 11

Meylan, G., Hauck, B.: 1981, *Astron. Astrophys. Suppl.* **46**, 281

Pendl, E.S., Seggewiss, W.: 1975, in *Physics of Ap-Stars*, *IAU Coll.* no. **32**, eds. W.W. Weiss, H. Jenkner, J.H. Wood, Univ. Wien, p. 357

Rufener, F.: 1989, *Astron. Astrophys. Suppl.* **78**, 469

Sanders, W.L.: 1971, *Astron. Astrophys.* **15**, 308

Schmidt, E.G.: 1978, *Publ. Astron. Soc. Pacific* **90**, 157

Smith, G.H.: 1983, *Publ. Astron. Soc. Pacific* **95**, 296

Smyth, M.J., Nandy, K.: 1962, *Publ. R. Obs. Ed.* **3** no. 2